Design of a Surgical Port for Minimally Invasive Beating-Heart Intracardial Procedures

Citation: DiBiasio, Christopher M. et al. "Design of a Surgical Port for Minimally Invasive Beating-Heart Intracardial Procedures." Journal of Medical Devices 5, 4 (2011): 045001 © 2011 American Society of Mechanical Engineers

As Published: http://dx.doi.org/10.1115/1.4004867

Publisher: ASME International

Persistent URL: http://hdl.handle.net/1721.1/120037

Version: Final published version: final published article, as it appeared in a journal, conference proceedings, or other formally published context

Design of a Surgical Port for Minimally Invasive Beating-Heart Intracardial Procedures

Christopher M. DiBiasio

Keith V. Durand

Jonathan Hopkins

Zach Traina

Alexander H. Slocum[1]
e-mail: slocum@mit.edu

Massachusetts Institute of Technology,
Department of Mechanical Engineering,
Cambridge, MA 02139

Nikolay V. Vasilyev

Pedro J. del Nido

Children's Hospital of Boston,
Department of Cardiac Surgery,
Boston, MA 02115

Direct-access, minimally invasive, beating-heart intracardial procedures have the potential to replace many traditional surgical procedures requiring cardio-pulmonary bypass as long as micro-emboli are prevented from entering the cardiovascular system. A new surgical port was developed to introduce surgical instruments into chambers of the beating heart during minimally invasive, intracardial surgical procedures without allowing the introduction of micro-emboli 0.1 mm or larger in size. The design consists of an outer port body that is secured to the heart wall using a purse string suture and a series of inner tubular sleeves that form the interface between the port and the transecting instrument. The design enables rapid tool changes and accommodates a wide variety of instruments. The port uses a fluid purging system to dislodge and remove emboli from a surgical instrument. Laboratory and clinical tests show that the port adequately seals around a surgical instrument and prevents the introduction of emboli with diameters greater than 0.1 mm into the heart while minimizing hemorrhage. [DOI: 10.1115/1.4004867]

1 Introduction

The advent of minimally invasive surgical procedures has led to a push for minimally invasive intracardiac procedures. One method of cardiac surgery [1–3] requires direct access to intracardiac structures while the heart is still beating. In order for such a procedure to be successful a surgical port must be developed that allows access to the inner structures of the heart without allowing air micro-emboli to be introduced into the cardio-vascular system [4]. Introduction of large air bubbles, specifically those easily detected by echocardiography (0.5 mm and larger), into the cardiac chambers has been associated with risk of stroke and injury to other organs [4]. Unfortunately no conventional surgical port is capable of preventing the introduction of micro-emboli into the heart cavity. Other investigators have proposed the use of modified thoracoscopic or laparoscopic surgical ports for intracardiac beating-heart image-guided intervention; however, these modified instruments could not be adopted in part due to the risk of introducing emboli during instrument introduction [5,6]. In this paper, we present the design of a beating-heart surgery compatible port that uses a purging system to remove air micro-emboli from surgical instruments inserted through the port.

Minimally invasive cardiac interventions can be performed via two different techniques: (1) catheterization [7] and (2) direct-access [1–3]. Catheterization involves the insertion of long flexible tools into the body via an access point (usually through the femoral vessels in the groin) and then snaking the tools through the cardio-vascular system until they reach the heart. These procedures allow for the repair of intracardial structures while the heart is still beating. However, trans-catheter procedures pose significant limitations. For example, often the patient must be large enough to allow catheterization since the diameter of the catheters is large compared to the blood vessels, and direct tissue manipulation is limited due to the lack of rigidity of catheters.

Direct-access, beating-heart surgical techniques would allow surgeons to repair intracardiac structures with greater facility and precision than current catheterization techniques allow. With this kind of procedure, one or more surgical ports could be placed in the heart to allow the introduction of a variety of surgical tools, imaging tools, and repair devices. Surgical ports could allow for an increase in the number of surgical trajectories, allowing access to a greater number of intracardiac structures, making this technique potentially more versatile than catheterization.

Current direct-access, minimally invasive intracardiac repairs rely on cardiopulmonary bypass (CPB) to allow access to the internal structures of the heart. Problems associated with CPB include the development of reperfusion disorders, heart muscle damage, and the potential for introduction of air emboli into the cardio-vascular system. Additional complications associated with CPB include: an inflammatory response from blood exposure to a foreign surface, bleeding, hypotension, sepsis, delayed wound healing, infection, and death [8,9].

Current surgical ports for thoracic surgery and other minimally invasive procedures are not compatible with the demands of beating-heart, intracardiac procedures. These surgical ports are designed to keep blood and other fluids in the body from exiting. They are not; however, designed to prevent emboli from entering the body cavity, a significant deficiency with respect to cardiac surgery.

2 Removal of Air Micro-Emboli

There are a limited number of methods for removing air emboli from instruments that are inserted into a surgical port. These methods include (1) buoyancy, (2) ultrasonic agitation, (3) wiping, and (4) fluid purging.

Embolus removal via buoyancy involves flooding an intermediate chamber with a fluid denser than the embolus (which is usually composed of air), thus allowing the embolus to float towards the top of the chamber. One potential danger is that if the surgical port is ever positioned such that the proximal end (where the instrument is inserted) is lower than the distal tip (where the instrument is introduced into the heart) emboli will float into the heart chamber.

Ultrasonic agitation can break up micro-emboli into a number of smaller emboli that are safe for introduction into the cardio-vascular system. This method would require an ultrasonic actuator be either integrated into the surgical port or easily attached to it. One danger with this method is the potential for the smaller emboli to coalesce into another large, dangerous micro-embolus. This coalescence is not easily controlled and therefore ultrasonic agitation must be combined with another method of embolus removal when used in practice.

[1]Corresponding author.

Manuscript received March 8, 2011; final manuscript received July 20, 2011; published online November 7, 2011. Assoc. Editor: Paul A. Iaizzo.

Wiping can help to remove emboli from an instrument before it enters the surgical port. By adding a compliant wiping seal such as an o-ring to the proximal end of the port it is possible for the instrument to have emboli removed as the instrument passes through the tight o-ring seal. However, if an instrument has a varying cross-section or is oddly-shaped, this method is ineffective. In addition, many surgical instruments are hollow and the wiping method is not capable of removing emboli from the interior of these instruments.

Fluid purging involves flooding an intermediate chamber in the port with a fluid such as saline or carbon dioxide and then either suctioning or driving the fluid under pressure through and around the surgical instrument. The induced flow of the flushing agent dislodges emboli from the exterior and interior of an instrument and then removes them from the surgical port. The one disadvantage of this method is that each instrument insertion requires a purging period of a few seconds.

While all four methods can be successful depending on the specific application, in general fluid purging is the most safe, reliable, and robust method for embolus removal. It was, therefore, chosen as the embolus removal method to be implemented in the surgical port design. Note that this does not preclude the addition of one or more of the other methods to be used in conjunction with the fluid purging system in later evolutions of the instrument.

3 Design of the Surgical Port

The design team included cardiac surgeons who worked closely with the mechanical engineers through a peer review design process [10] to develop the new surgical port. The first step was to define the problem and identify the primary functional requirements of the surgical port:

(1) Allow direct access for various surgical tools into the chambers of the heart
(2) Prevent entry of air micro emboli greater than 0.5 mm into the heart
(3) Minimize damage to heart tissues and other organs
(4) Minimize blood loss from the heart

The central function of the port is to allow surgical tools of various shapes and sizes to gain entry into the interior of the heart both safely and quickly. The second primary requirement, which drives the need for a new type of surgical port, is to prevent micro-emboli (usually air) of diameters greater than 0.5 mm air from entering the chambers of the heart during the surgery. Doing this requires the removal of air from tools entering the heart as well as sealing off the incision and surgical port to the atmosphere while tools are being removed or changed. The surgical port must also have a small cross-section in order to allow it to be inserted between a patient's ribs and minimize the required incision in the heart wall. Finally, the surgical port must limit the amount of blood lost during its insertion and during its operation.

3.1 Surgical Port Operation. A small incision is made in the thoracic wall that allows direct access to the heart via a trajectory located in between a patient's ribs. A purse-string suture is placed in the wall of the heart in the chamber of interest. The surgical port, shown in Fig. 1(*a*) and 1(*b*), is inserted in the incision and through the wall of the heart with the aid of a trocar or obturator.

The purse string suture seals the heart wall tissue around the heart tissue anchors located on the outer diameter of the distal end of the surgical port body. A tool sleeve, which has a standardized outer diameter and whose bore is customized for a particular surgical instrument, is then inserted into the surgical port body. The surgical instrument is then inserted into the tool sleeve and then pushed forward until the distal tip of the instrument has just

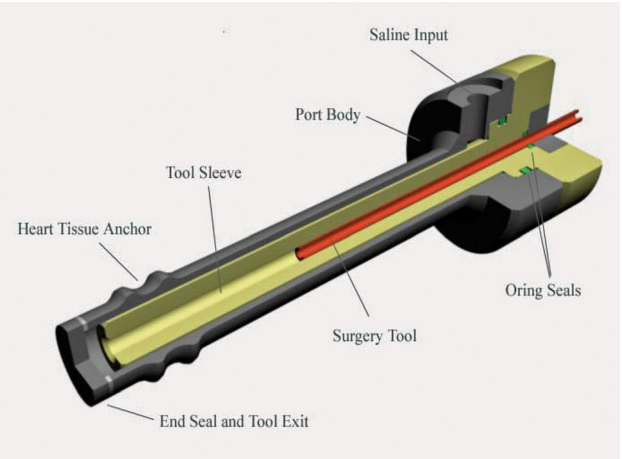

(a)

(b)

Fig. 1 Solid model (*a*) and as fabricated (*b*) surgical port

reached the end seal located at the distal end of the surgical port body. This concludes the insertion and assembly of the surgical port into the patient.

In order to begin the purging cycle a differential pressure is applied, usually by a standard wall suction source in the operating room. The suction is applied through the instrument and/or around the instrument via the tool sleeve. This induces the flow of a flushing agent such as saline to flow from a reservoir and through the gap between the port body and tool sleeve. Fluid is allowed to circulate through the surgical port and instrument for approximately five seconds at which time the differential pressure is removed, stopping flow. The surgical instrument has now been cleaned and only now may pass through the end seal and into the heart.

3.2 Surgical Port Design Details. Many of the design decisions for the surgical port, such as a custom tool sleeve, may seem arbitrary but are crucial to the removal of micro-emboli from surgical instruments via the surgical port. Engineering a flexural seal capable of adequately sealing the wide range of tool sizes (1–5 mm in diameter) used in intracardial surgical procedures proved to be challenging. Tool sleeves dedicated to a particular surgical instrument were designed so as to standardize the mating interface between the surgical port body and each instrument tool sleeve. By custom sizing the bore and instrument seal of every tool sleeve for a particular surgical instrument it can be assured that the seal around each surgical instrument was secure and robust regardless of the variance in the shapes and sizes of the surgical instruments and devices selected. Thus, the surgical port body was designed with a fixed bore into which tool sleeves for a particular surgical instrument

could be easily and rapidly inserted while the surgical port body was still attached and sealed to the heart wall.

The tool sleeve is secured to the surgical port body via an o-ring as shown in Fig. 1, though a variety of sealing options could be used. The authors successfully demonstrated interference fits between a PVDF surgical port body and a PTFE tool sleeve that showed no leakage when driven by operating room suction. Note that PDF is a preferred surgical port body material due to its 3D echocardiograph visibility. In production, it may be possible to replace the o-ring with a series of flexural ribs that could be molded onto the outer diameter of the tool sleeve. For simplicity of design the seal between the surgical instrument and tool sleeve is provided by an o-ring, though either of the two aforementioned sealing methods could be used.

3.3 End Seal Design Details. Original prototypes of the instrument body included a magnetically preloaded flexible flap valve at the tip of the device. While this compliant flap valve adequately sealed during embolus removal, the door opening mode of a flap seal carried the risk of flap failure creating a loose foreign body in the heart. There was also the practical issue concerning device work volume. During initial tests of the instrument in a porcine model, the flap valve performed well.

There are many types of passive flexural structures that allow for needles to be inserted for aspirating or injecting fluids into a sample chamber, such as a simple diaphragm with cross slits. However, the functional requirement of minimal blood loss meant that the valve must resist the pressure spikes from the beating heart. In addition, when blood pressure is low between beats the fluid purging pressure must not flood the heart with saline. A duckbill valve was considered, but its required footprint to maximum tool diameter ratio was too large. The team finally decided on a trileaflet valve design [11], shown in Fig. 2, which was prototyped by molding a small silicon rubber cone and then using a fixture to cut slits in it to form the valve. It took several attempts but the result was a robust valve that satisfied the functional requirements.

(a)

(b)

Fig. 2 Trileaflet end seal design in the (*a*) closed and (*b*) open positions

4 Fluid Modeling for the Port

In order to prevent the intracardial entry of emboli the dimensions of the port must be selected to establish the proper flow rate through the various cavities of the port. This can be done by modeling the fluid network for the instrument to link the geometry of the port and fluid properties to the fluid flow rate.

4.1 Fluid Flow Requirements. The minimum flow rate in the port is dependent on three different requirements: (1) minimum flow speed required to separate an embolus from a wall, (2) minimum flow speed required to overcome the buoyancy force of an embolus, and (3) ensuring the minimum local pressure to prevent cavitation is exceeded. The force required to remove an embolus from the wall of the port depends on the surface tension between the wall and the embolus, σ, the radius of the embolus, a, and the speed of the flow around the embolus, U. The maximum force needed to remove an embolus from a surface, F_σ, occurs if the embolus takes the form of a hemisphere on the wall:

$$F_\sigma = 2\pi a\sigma \tag{1}$$

This force is opposed by the drag force, F_D, from a half sphere, which we estimate as half of the standard Stoke's drag solution for a sphere:

$$F_D = 3\pi\mu_{flow}aU \tag{2}$$

From Eqs. (1) and (2) the minimum free flow velocity to dislodge an embolus from the wall in saline is determined to be 9.3 mm/sec. Equations (1) and (2) assume the materials used to construct the port body are hydrophilic; thus making a more conservative approximation of the force needed to dislodge an embolus from the wall of the port. The materials actually used in the port, PVDF, are hydrophobic, adding a factor of safety to the design.

Fluid flow completely changes direction in the flow channels located in the instrument body and in the tool sleeve. This design, therefore, necessitates the need for the fluid to be moving fast enough to overcome the buoyancy force of an embolus rising in a column of fluid. Equation (3) relates the necessary free flow speed of the fluid to the density and viscosity of the flow fluid, ρ_{flow} and μ_{flow}, to the density and viscosity of the embolus, $\rho_{embolus}$ and $\mu_{emboilus}$, as well as gravitational acceleration, g.

$$U = \frac{2}{3}\left(\frac{a^2 g(\rho_{embolus} - \rho_{flow})}{\mu_{flow}}\right)\left(\frac{\mu_{flow} + \mu_{embolus}}{2\mu_{flow} + 3\mu_{embolus}}\right) \tag{3}$$

For a 1 mm embolus (corresponding to the largest embolus seen in tank and clinical tests) the minimum flow velocity required through the port is 0.83 m/s. This flow velocity is larger than the minimum found from Eq. (1) and (2), therefore it becomes the conservative minimum flow speed for the port flow path.

It is possible for emboli to be introduced into the port via cavitation of the flushing fluid. If the local absolute pressure at any point in the port falls below saline's vapor pressure, the water in the saline solution will undergo a phase change leading to the creation of emboli composed of water vapor and other gases dissolved in the saline solution. Saline's vapor pressure at body temperature is 5.0 kPa. The port dimensions where chosen to ensure that the local absolute pressure in the port was never allowed to drop below 10 kPa.

4.2 Port Fluid Flow Model. The analysis presented in Sec. 4.1 provides the minimum guidelines for flow speed and local pressure in the instrument. This section will create a model that links these local parameters with the port geometry, fluid properties, and the global pressure differential applied via operating room suction. The applied pressure differential, ΔP, is related to the total flow rate, Q, and the flow resistance of the inlet hose,

R_{inlet}, outlet hose, R_{outlet}, gap between the port body and tool sleeve, R_{port}, and the flow channel in the tool, R_{tool}, as shown in Eq. (4).

$$\Delta P = \left(R_{inlet} + R_{outlet} + R_{port} + R_{tool}\right)Q \tag{4}$$

The tubing we are using for supply and drain of the saline is approximately 0.3 cm in diameter. Using 1 m/s as the characteristic speed of the flow, we find the supply and drain tubes have a Reynolds number of 2500, which is in the transition region between turbulent and laminar flow, allowing us to still use the Hagen-Poiseuille relations in Eqs. (5) and (6) to define the inlet and outlet resistance as a function of hose diameter, D, and hose length, L.

$$R_{inlet} = \frac{128\mu_{saline}L_{inlet}}{\pi D_{inlet}^4} \tag{5}$$

$$R_{outlet} = \frac{128\mu_{saline}L_{outlet}}{\pi D_{outlet}^4} \tag{6}$$

The flow resistance of the tool is found in a similar manner as for the inlet and outlet hoses. Its resistance is found via Eq. (7).

$$R_{tool} = \frac{128\mu_{saline}L_{tool}}{\pi D_{tool}^4} \tag{7}$$

The flow resistance of the gap between the tool sleeve and port body is modeled as Poiseuille flow between two flat plates. This holds as long as the gap between the tool sleeve and port body, h_{gap}, is less than 1% of the port body inner diameter, D_{body}. Equation (8) relates the port resistance to the port geometry, including the port body length, L_{body}.

$$R_{port} = \frac{12\mu_{saline}L_{body}}{\pi D_{body}h_{gap}^3} \tag{8}$$

Combining Eqs. (4)–(8) with the fluid flow constraints found in Sec. 4.1 allows the geometry of the port to be determined. Table 1 shows the relevant dimensions and performance metrics of the port. Note, P_{min} corresponds to the lowest pressure in the port relative to atmospheric pressure and U_{min} corresponds to the lowest flow speed in the port. Note that the minimum required flow rate and absolute pressures were maintained in the port via the chosen port geometry.

5 Port Testing

It was necessary to perform a combination of ex vivo and in vivo tests to verify the port's operation with a beating heart. An ex vivo laboratory test was conducted in a tank of water while the distal end was visualized via ultrasound in order to quantify the number and size of emboli introduced through the port. The in vivo tests were conducted on a live porcine heart and imaged with a 3D ultrasonic probe.

Table 1 Relevant Port Parameters

h_{gap}	0.35	mm
L_{tool}	18	cm
L_{body}	6.8	cm
D_{tool}	2.1	mm
D_{body}	8	mm
D_{inlet}	0.32	mm
D_{outlet}	0.32	mm
ΔP	180	mm Hg
Q	8.5	mL/sec
P_{min}	879	Pa (gage)
U_{min}	1.02	m/s

5.1 Ex Vivo Ultrasonic Image Testing. The first test on the prototype utilized ultrasonic imaging to determine the presence and size of emboli introduced from the port during tool insertion. During the tests the barrel of the port body was submerged in a tank of water held at body temperature (37 C) and degassed via use of a SONOS 7500 Ultrasound System with an X4 Matrix Transducer (Philips Healthcare, Andover, MA). This particular imaging system allowed visualization of air emboli 0.1 mm in diameter and larger. After letting the tank stabilize overnight, 150 tool insertions were sequentially performed while an ultrasonic probe was used to inspect the tip of the tool and the instrument body for released or attached emboli.

Tool insertions were performed in six groups of 25 insertions. The procedure for each group of twenty-five tool insertions consisted of first removing the tool sleeve from the port body and then reinserting the tool sleeve into the port body. A tool was then inserted into the tool sleeve and a five second purging cycle was applied. The tool tip was then inserted through the tri-leaflet seal where both the distal end of the port body and the tool tip were

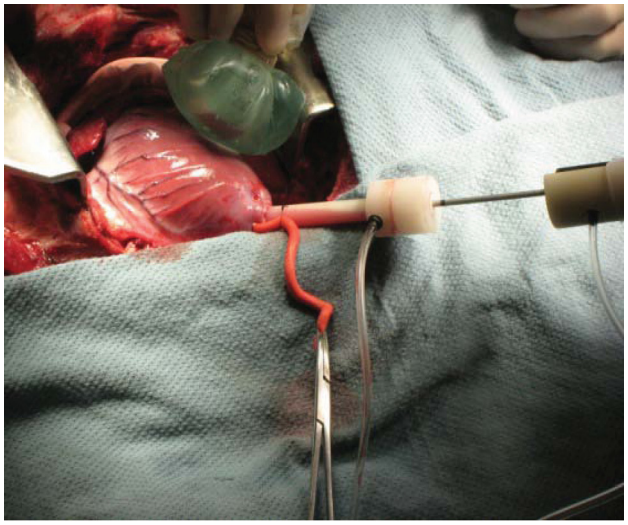

(a)

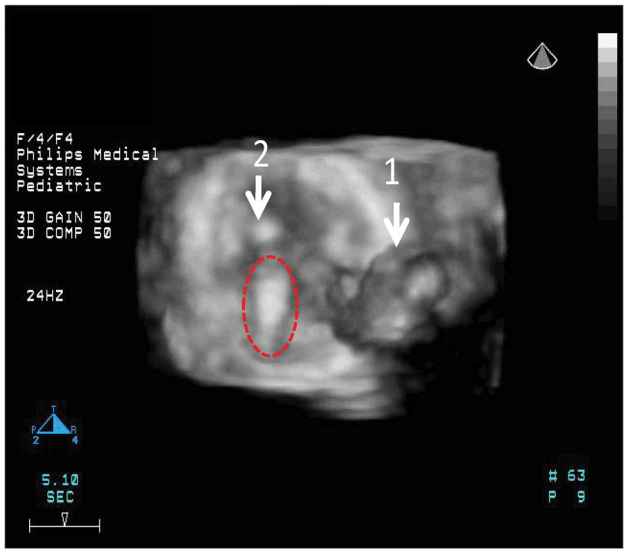

(b)

Fig. 3 Images of the (*a*) in vivo experiments used to validate the port operation and (*b*) bubbles introduced with flushing system disabled. The tip of port [1], the tip of the tool [2], and an embolus (dashed oval) are clearly visible in the ultrasound image.

inspected via ultrasound for emboli. After inspection the tool was then completely withdrawn for the port and then reinserted using the same flushing procedure until twenty-five tool insertions had been reached. During the course of the 150 insertions no emboli were observed on the distal end of the tool, the tri-leaflet valve, the port body, the tool tip, or in the surrounding fluid. In order to establish a baseline, the system was also tested without the five second purging step. During these tests emboli over 0.5 mm in diameter were present during every single insertion; thus verifying the need for the flushing system and proving its effectiveness.

5.2 In Vivo Testing. In vivo testing of the port during an actual procedure was performed, as shown in Fig. 3(*a*), to further evaluate the port's performance. The in vivo tests were performed on a swine model using an experimental protocol approved by the Children's Hospital Boston Institutional Animal Care and Use Committee. The main goals of these in vivo trials were to (1) test the effectiveness of the insertion/anchoring procedure and (2) test the effectiveness of the port flushing system.

To test the effectiveness of the insertion/anchoring procedure the port was introduced into the cardiac chambers, anchored, and left for 30 mins in order to test the integrity of the end seal and port anchoring design. At no point did any of the purse string sutures or end seals leak after installation during this thirty minute trial, even in the presence of the large pressure differential provided by the left ventricle. This confirmed the integrity of both the end seal design as well as the port anchoring mechanism. Note that the port was inserted into the other chambers of the heart with similar results.

The next experiment tested the effectiveness of the port flushing system in removing emboli. In order to ensure compatibility with the new port flushing system, standard surgical instruments were modified to allow suction to be drawn through the instrument body. To test the flushing system the tools were inserted over 50 times while the tip of the tool and port was imaged via SONOS 7500 Ultrasound System with an X4 Matrix Transducer (Philips Healthcare, Andover, MA). This particular imaging system also allowed visualization of air emboli 0.1 mm in diameter and larger. When the flushing system was enabled and used before every instrument insertion there was no visual evidence of emboli being introduced into the heart chamber via the surgical instruments or the port. In contrast, when the flushing system was disabled and the tool inserted newly introduced emboli were visible, as shown in Fig. 3(*b*). In Fig. 3(*b*) the tip of the port is labeled as 1, the tip of the instrument is labeled as 2, and an air embolus is denoted by the dashed oval. This confirms that the port flushing system is capable of reducing the introduction of emboli from surgical tools.

6 Conclusion

A surgical port was developed for intracardial access of surgical instruments used in minimally invasive beating heart intracardial surgery. Several methods for preventing/eliminating emboli from being introduced during tool insertion were discussed. A flushing system was developed for the surgical port and operating conditions and design equations for its implementation were introduced. Ex vivo and in vivo testing with an ultrasound probe visually verified that air emboli with diameters greater than 0.1 mm were not being introduced when the fluid flush system was implemented. In contrast, when the flushing system was disabled emboli with diameters of over 0.5 mm were routinely visualized. In vivo experiments verified the purse string suture attachment method as well as proper operation in an animal test environment. There were no signs of blood leakage/seepage during the in vivo tests. The surgical port was used to enter the ventricular and atrial chambers of the heart and allowed successful instrument manipulation inside the beating heart.

Further work will focus on integrating optics into the port body for enhanced visualization at the distal end of the port. This would allow visualization of intracardial structures via an endoscope in addition to the 3D ultrasound images collected during surgical procedures.

Acknowledgment

This material is based upon work supported by the Center for Integration of Medicine and Innovative Technology (CIMIT www.cimit.org). The authors would also like to acknowledge Dr. Jennifer White for her advice on designing the trileaflet valve.

References

[1] Walther, T., Simon, P., Dewey, T., Wimmer-Greinecker, G., Falk, V., Kasimir, M. T., Doss, M., Borger, M. A., Schuler, G., Glogar, D., Fehske, W., Wolner, E., Mohr, F. W., and Mack, M., 2007, "Transapical Minimally Invasive Aortic Valve Implantation: Multicenter Experience," Circulation, **116**, pp. I240–I245.

[2] Bajona, P., Katz, W. E., Daly, R. C., Zehr, K. J., and Speziali, G., 2009, "Beating-Heart, Off-Pump Mitral Valve Repair by Implantation of Artificial Chordae Tendineae: An Acute In Vivo Animal Study," J. Thorac. Cardiovasc. Surg., **137**(1), pp. 188–193.

[3] Vasilyev, N. V., Melnychenko, I., Kitahori, K., Freudenthal, F. P., Phillips, A., Kozlik-Feldmann, R., Salgo, I. S., del Nido, P. J., and Bacha, E. A., 2008, "Beating-Heart Patch Closure of Muscular Ventricular Septal Defects Under Real-Time Three-Dimensional Echocardiographic Guidance: A Preclinical Study," J. Thorac. Cardiovasc. Surg., **135**(3), pp. 603–609.

[4] Stump, D. A., Kon, N. A., Rogers, A. T., and Hammon, J. W., 1996, "Emboli and Neuropsychological Outcome Following Cardiopulmonary Bypass," Echocardiography, **13**(5), pp. 555–558.

[5] Suematsu, Y., Marx, G. R., Triedman, J. K., Mihaljevic, T., Mora, B. N., Takamoto, S., and del Nido, P. J., 2004, "Three-Dimensional Echocardiography-Guided Atrial Septectomy: An Experimental Study," J. Thorac. Cardiovasc. Surg., **128**(1), pp. 53–59.

[6] Downing, S. W., Herzog, W. A., Jr., McLaughlin, J. S., and Gilbert, T. P., 2002, "Beating-Heart Mitral Valve Surgery: Preliminary Model and Methodology," J. Thorac. Cardiovasc. Surg., **123**(6), pp. 1141–1146.

[7] Leon, M. B., Kodali, S., Williams, M., Oz, M., Smith, C., Stewart, A., Schwartz, A., Collins, M., and Moses, J. W., 2006, "Transcatheter Aortic Valve Replacement in Patients With Critical Aortic Stenosis: Rationale, Device Descriptions, Early Clinical Experiences, and Perspectives," Semin. Thorac. Cardiovasc. Surg., **18**(2), pp. 165–174.

[8] Roth-Isigkeit, A., Hasselbach, L., Ocklitz, E., Bruckner, S., Ros, A., Gehring, H., Schmucker, P., Rink, L., and Seyfarth, M., 2001, "Inter-Individual Differences in Cytokine Release in Patients Undergoing Cardiac Surgery With Cardiopulmonary Bypass," Clin. Exp. Immunol., **125**(1), pp. 80–88.

[9] Antonelli, M., Testa, G., Tritapepe, L., D'Errico, R. R., Costa, D., Giovannelli, L., Riccioni, L., Gasparetto, A., and Catena, G., 1999, "IL-8, IL-6 and ICAM-1 in Serum of Paediatric Patients Undergoing Cardiopulmonary Bypass With and Without Cardiocirculatory Arrest," J. Cardiovasc. Surg., **40**(6), pp. 803–809.

[10] Graham, M., Slocum, A., and Sanchez, R., 2007, "Teaching High School Students and College Freshmen Product Development by Deterministic Design With PREP," J. Mech. Des., **129**(7), pp. 677–681.

[11] White, J., Agnihotri, A., Latrémouille, C., Messas, E., Carpentier, A., and Torchiana, D., 2005, "A Method of Using the Pulmonary Trunk to Form a Trileaflet Valve," J. Thorac. Cardiovasc. Surg., **129**(3), pp. 677–679.